Endogenous secretory receptor for advanced glycation end-products inhibits amyloid-β 1-42 uptake into mouse brain

著者	Sugihara Takahiro, Munesue Seiichi, Yamamoto Yasuhiko, Sakurai Shigeru, Akhter Nasima, Kitamura Yoji, Shiba Kazuhiro, Watanabe Takuo, Yonekura Hideto, Hayashi Yasuhiko, Hamada Jun-ichiro, Yamamoto Hiroshi
journal or publication title	Journal of Alzheimer's Disease
volume	28
number	3
page range	709-720
year	2012-01-01
URL	http://hdl.handle.net/2297/30370

doi: 10.3233/JAD-2011-110776

Endogenous Secretory Receptor for Advanced Glycation End-products Inhibits Amyloid-β_{1-42} Uptake into Mouse Brain

Takahiro Sugihara[1], Seiichi Munesue[1*], Yasuhiko Yamamoto[1*], Shigeru Sakurai[1], Nasima Akhter[2], Yoji Kitamura[2], Kazuhiro Shiba[2], Takuo Watanabe[1], Hideto Yonekura[3], Yasuhiko Hayashi[4], Jun-ichiro Hamada[4], and Hiroshi Yamamoto[1]

[1]Department of Biochemistry and Molecular Vascular Biology, Graduate School of Medical Science, and [2]Division of Tracer Kinetics, Advanced Science Research Center, Kanazawa University, Kanazawa 920-8640, Japan
[3]Department of Biochemistry, Kanazawa Medical University School of Medicine, Uchinada 920-0293, Japan
[4]Department of Neurosurgery, Graduate School of Medical Science, Kanazawa University, Kanazawa 920-8640, Japan

*Corresponding authors: Seiichi Munesue and Yasuhiko Yamamoto, Department of Biochemistry and Molecular Vascular Biology, Kanazawa University Graduate School of Medical Science, 13-1 Takara-machi, Kanazawa 920-8640, Japan. Tel.: +81-76-265 -2181; Fax: +81-76-234-4217; E-mail: smunesue@med.kanazawa-u.ac.jp and yasuyama@med.kanazawa-u.ac.jp

Abstract

The cell-surface receptor for advanced glycation end-products (RAGE) has been implicated in the development of diabetic vascular complications and Alzheimer's disease. RAGE has been considered to be involved in amyloid-β_{1-42} ($A\beta_{1-42}$) uptake into brain. In the present study, we demonstrate that endogenous secretory RAGE (esRAGE), a decoy form of RAGE generated by alternative RNA processing, is able to inhibit $A\beta_{1-42}$ influx into mouse brain. Surface plasmon resonance and competitive binding assays revealed that human $A\beta_{1-42}$ interacted with human esRAGE within the immunoglobulin V type region. We next examined the uptake and distribution of ^{125}I-labeled human $A\beta_{1-42}$ in various organs and body fluids of newly created mice overexpressing human esRAGE as well as RAGE-null and wild-type (WT) mice. The transition of the ^{125}I-labeled $A\beta_{1-42}$ from circulation to brain parenchyma peaked at 30 min after the injection into WT mice, but this was significantly blunted in esRAGE-overexpressing and RAGE-null mice. Brain regions where significant reduction in ^{125}I-labeled $A\beta_{1-42}$-derived photo-stimulated luminescence were marked in ventricles, cerebral cortex, hippocampus, especially CA1 and CA3 regions, putamen, and thalamus. The results thus suggest the potential of esRAGE in protection against the development of Alzheimer's disease.

Key words: RAGE, esRAGE, transgenic mice, $A\beta_{1-42}$, Alzheimer's disease

Introduction

Receptor for advanced glycation end-products (RAGE) is a pattern recognition receptor, which binds to not only advanced glycation end-products (AGE) [1], but also S100/calgranulins [2], Mac-1 [3], transthyretin [4], high mobility group box-1 (HMGB-1)/amphoterin [5], lipopolysaccharides (LPS) [6], phosphatidylserine [7], and amyloid-β (Aβ) [8]. Interactions of these diverse ligands with RAGE contribute to various pathologic processes including diabetic complications [9, 10], proinflammatory reactions, tumor progression, efferocytosis, and Alzheimer's disease (AD) [11, 12].

The presence of senile plaque formed by extracellular amyloid depositions and that of intracellular neurofibrillary tangles composed of hyperphosphorylated tau proteins are the major pathological hallmarks of AD [13]. The predominant forms of non-fibrillar Aβ that give rise to amyloid plaques are $A\beta_{1\text{-}40}$ and $A\beta_{1\text{-}42}$ fragments [14]. While soluble $A\beta_{1\text{-}40}$ is the major form of circulating Aβ and cerebrovascular amyloid, the major constituent of amyloid plaques is $A\beta_{1\text{-}42}$. $A\beta_{1\text{-}42}$ rapidly forms oligomers at very low concentrations, and thus has been regarded as the major cause of neurotoxicity at an early stage of AD [15]. Monomeric $A\beta_{1\text{-}40}$ is reported to have neuroprotective effects against $A\beta_{1\text{-}42}$-induced neuronal damage [16, 17].

Transport of peptides at the blood-brain barrier (BBB) requires a receptor- or carrier-mediated transport system [18]. Unrestricted diffusion readily occurs across the capillaries in peripheral organs, such as the heart, but not across the BBB [19]. Studies using an *in vitro* model of BBB showed that RAGE mediated the binding of soluble $A\beta_{1\text{-}40}$ at the apical side of brain capillary endothelium, and that RAGE was involved in $A\beta_{1\text{-}40}$ transcytosis [20]. Low-density lipoprotein receptor-related protein-1 (LRP-1) is also known to participate in the receptor-mediated flux of Aβ across BBB [21, 22]. LRP-1 appears to mediate the efflux of Aβ from the brain to the periphery, whereas RAGE is implicated in Aβ influx back into the CNS [22]. Deletion of the RAGE gene eliminates the transport of free circulating Aβ into the brain [23]. Giri *et al.* reported that RAGE is also involved in $A\beta_{1\text{-}40}$-mediated migration of monocytes across BBB [24].

RAGE has multiple isoforms both in human and mouse. Membrane-bound RAGE transduces intracellular signaling upon ligand engagement on the cell surface. Soluble forms of RAGE act as decoy receptors in the extracellular space [25-29]. Soluble forms of RAGE can be generated by the following two mechanisms; one is alternative splicing of RAGE transcripts [25], and the other is ectodomain shedding [26-29]. We isolated the former variant which is stably present in human blood and named it endogenous

secretory RAGE (esRAGE). esRAGE is capable of capturing ligands, thereby protecting cells from ligand-induced injury [25]. Immunohistochemical analysis with RAGE domain-specific antibodies revealed that expression of esRAGE could be higher than that of membrane-bound RAGE in human brain [30]. We also showed lower expression of esRAGE in hippocampal CA1 region of AD brain than that of non-AD brain [31].

These observations have prompted us to determine whether a higher concentration of circulating esRAGE could exert a protective effect against AD. In the present study, we first confirmed human $A\beta_{1-42}$-esRAGE interaction, then created human esRAGE-overexpressing transgenic (Tg) mice, and compared ^{125}I-labeled $A\beta_{1-42}$ influx into the brain among wild-type (WT), esRAGE Tg and RAGE-null mice.

Materials and Methods

Chemicals

Human $A\beta_{1-42}$ peptides for surface plasmon resonance (SPR) and radiolabeling were purchased from Sigma-Aldrich Inc. (St. Louis, MO, USA) and Peptide Instutute (Osaka, Japan), respectively. FAM-labeled $A\beta_{1-42}$ peptide for competitive binding assay was from AnaSpec Inc. (Fremont, CA, USA) and [^{125}I]sodium iodide (NEZ-033A; >600 GBq/mg) was from PerkinElmer Inc. (Waltham, MA, USA).

Human esRAGE-specific antibody used for western blot analysis of sera and for ELISA was immunoaffinity-purified rabbit anti-human esRAGE-specific polyclonal antibody raised against the unique C-terminal 16-amino-acid peptide (amino acids 332–347; EGFDKVREAEDSPQHM) [25]. This antibody recognizes human but not mouse esRAGE. Pan-RAGE antibody for western blot analysis of brain was goat anti-RAGE antibody raised against synthetic peptide that corresponds to amino acids 42-59 of human RAGE (Millipore). This antibody recognizes both membrane-bound RAGE and esRAGE of either human or mouse origin.

Animals

Human esRAGE Tg mice were created as follows. A 1,044-bp fragment of human esRAGE cDNA, mouse albumin enhancer/promoter (National Cancer Institute, USA) [32], human β-globin intron, and SV40 late poly(A) region were used for the construction of a transgene (Fig. 2A). The transgene was injected into fertilized BDF1 ova for production of the Tg mice (Japan SLC, Inc.). Germline transmitted Tg mice were then backcrossed into C57BL6/J (>7 generations), and the heterozygous Tg mice were used in the current study. Genotyping was carried out by PCR analysis with the following primers corresponding to the region of the albumin enhancer/promoter: forward, 5'-GCTTGGCTTGAACTCGTT-3' and reverse, 5'-GCTACCTTAAAGATCCCG-3'. The transgene-carrying allele yielded a band at 404 bp on agarose gel electrophoresis.

The esRAGE Tg mice, RAGE-null mice developed in our lab [33], and WT C57BL/6J mice (Charles River, Yokohama, Kanagawa, Japan) were housed in a pathogen-free barrier facility and maintained on normal rodent chow with free access to food and water. Male mice at 8~16 weeks of age were used for all experiments. Animals were treated in accordance with the Fundamental Guidelines for Proper Conducts of

Animal Experiment and Related Activities in Academic Research Institutions under the jurisdiction of the Ministry of Education, Culture, Sports, Science, and Technology of Japan. The protocols for animal experiments were approved by the Institutional Animal Care and Use Committee of Kanazawa University.

SPR assay

Human esRAGE protein purified from conditioned media of COS7 cells, which had been stably transformed with esRAGE cDNA-expression vector [25], or $A\beta_{1\text{-}42}$ peptide was immobilized onto BIAcore CM5 research grade sensor chips by the amine coupling method in accordance with the supplier's recommendations. Human esRAGE and $A\beta_{1\text{-}42}$ peptide bindings to the immobilized $A\beta_{1\text{-}42}$ peptide and esRAGE protein, respectively, were examined with BIAcore 2000 system as described previously [6]; the flow buffer used contained 10 mM HEPES (pH 7.4), 0.15 M NaCl, 3 mM Na-EDTA, and 0.005% (v/v) surfactant P-20. Association and dissociation were measured at 25°C at a flow rate of 20 μL/min. The sensor chips were regenerated by washing with 10 mM NaOH and 0.5% (w/v) SDS. Kinetic parameter was obtained by fitting the sensorgrams to a 1:1 (Langmuir) binding model using the BIAevaluation 3.1 software.

Solid-phase reconstitution of a receptor-ligand binding and competition assay

One hundred μg of FAM-labeled $A\beta_{1\text{-}42}$ peptide were dissolved in 50 μL of 1% NH_4OH, dispensed into aliquots and stocked frozen at -20°C. The stocked $A\beta_{1\text{-}42}$ solution was diluted with phosphate-buffered saline (PBS) and used for assay. Each well of a 96-well ELISA plate (437915, Nalgene Nunc) was coated with 50 ng of purified human esRAGE proteins in 100 μL of PBS, and received 200 μL of 1 ng/μL FAM-labeled $A\beta_{1\text{-}42}$ peptide together with varying concentrations of the liquid-phase competitor esRAGE proteins. After incubation for 1 hr at 25°C, wells were washed three times with PBS and underwent the measurement of fluorescence at exitation/emission = 485/538 nm using a Fluoroskan Ascent FL (Labotal Scientific Equipment Ltd., Abn Gosh, Israel). The ligand binding and competition assay system has been successfully applied to other RAGE ligands, including AGE themselves [33].

Western blot analysis

Extraction of RAGE proteins from brain in esRAGE Tg, RAGE-null, and WT

mice were performed as previously described [34]. One μl each of sera from esRAGE Tg, RAGE-null, and WT mice or 10 μl each of affinity-purified brain extracts from esRAGE Tg, RAGE-null, and WT mice were loaded. Proteins were separated by SDS-PAGE (12.5%) and electroblotted onto PVDF membranes (Millipore). The membranes were blocked with 5% (w/v) non-fat dried milk in PBS and 0.1% (v/v) Tween 20, and then incubated with 0.5 μg/mL of rabbit anti-human esRAGE-specific polyclonal antibody [25] or 1,000-fold diluted goat pan-RAGE antibody (Millipore). Anti-Rabbit IRDye 680 and 800 were diluted 10,000-fold and used as the secondary antibody. The antigen-antibody complex was visualized using the Odyssey Infrared Imaging systems (LI-COR Biotechnology, Linclon, Nebraska, USA). Quantification of the intensity of immunoreacted bands was performed with the public domain Image J program in the 256-grayscale mode.

ELISA

ELISA kit (B-Bridge International, Inc) was employed to determine serum levels of human esRAGE in esRAGE Tg, RAGE-null and WT mice as described previously [35]. The ELISA system is not interfered by an addition of ligands.

Radioiodination of Aβ_{1-42}

Human Aβ_{1-42} peptides were labeled with ^{125}I by the method of chloramine-T as described previously [36-38]. Labeling and HPLC purification were carried out at Advanced Science Research Center, Kanazawa University. In brief, a solution containing human Aβ_{1-42} (10 μg/10 μL) and [^{125}I]sodium iodide (0.5 mCi/5 μL: 0.343 mCi/8 μL) were mixed in 85 μL of 0.2 M PBS (pH7.4) on ice. Chloramine-T (10 μL, 3.8 mM) was added to the solution, followed by agitation every 1 min. After 5 min, the reaction was terminated by adding $Na_2S_2O_5$ to a final concentration of 2.5 mM.

The reaction mixture (total: 165 μL) was applied onto a Zorbax 300 Extend-C18 (4.6 mm inner diameter x150 mm length) column equilibrated with TBS (pH 7.4) at a 1 ml/min flow rate at 45°C, and separated with the ^{125}I radioactivity and the absorbance at 220 nm being constantly monitored. The eluates were fractionated into glass tubes (2~4 mL/tube). Fractions containing labeled Aβ_{1-42} were collected and further separated in the same column but using a 20-60% linear gradient of acetonitrile in 0.1% TFA and a flow rate of 1 ml/min. After the chromatography, the solvent in the glass tube was evaporated under nitrogen gas. The recovery of the radioactivity was 91.3%. Purity of

the radiolabeled peptides was evaluated by paper chromatography. The ratio of the radioactivity incorporated into amyloid peptides/the radioactivity loaded on the paper chromatography was 2,697.90 x 10^3 cpm/2,733.99 x 10^3 cpm = 98.7%. When the ratio was greater than 95%, the radiolabeled material was considered pure enough to be used for biological analyses; the purified peptides were initially dissolved in DMSO, diluted to a concentration of 1 mg/mL in TBS, and analyzed for degree of oligomerization by SDS-PAGE. The final radioactivity associated with ^{125}I-labeled A$\beta_{1\text{-}42}$ was estimated to be 224 μCi/300 μL. ^{125}I-labeled A$\beta_{1\text{-}42}$ was stored at -20°C.

Biodistribution

Three groups of C57Bl/6J mice (n=6) were anesthetized with ether and received an intravenous bolus injection of 2 μCi of ^{125}I-labeled A$\beta_{1\text{-}42}$ in 0.2 mL of 0.1% BSA solution (91 nM as A$\beta_{1\text{-}42}$ concentration). After injection, the animals were euthanized at different time point intervals (5, 15, 30, 60, and 120 min). Immediately after blood samples were drawn and collected, the blood was washed out of the vascular system by infusing 30 mL of 0.1 M PBS (room temperature) at ~6 mL/min through a needle inserted into the left ventricle. Blood, brain, lung, liver, kidney, urine, and gallbladder were then collected, and weighed at each time point. The radioactivities were measured with a γ-counter (Aloka, ARC-1000, Tokyo), and total cpm were recorded. The resultant cpm was normalized to be cpm per gram of wet tissue and is expressed as % dose/g tissue.

***In vivo* autoradiography**

A hundred μCi of ^{125}I-labelled A$\beta_{1\text{-}42}$ tracer (4.6 μM as A$\beta_{1\text{-}42}$ concentration) was injected into the tail vein. At 30 min after the injection, animals were euthanized and blood vessels were immediately perfused. Then, the brain was quickly removed, fixed using Tissue-Tek (Sakura Finetek Japan Co., Ltd., Tokyo, Japan) and kept frozen in powdered dry ice. Serial coronal sections containing the hippocampus or cerebellum were exposed to tritium-imaging plate for 1 week. To quantitatively evaluate the autoradiograms, photo-stimulated luminescence (PSL) values were assessed using the Bio-Imaging Analyzer System (Fuji Film, Hamamatsu, Japan). Regions of interest (ROIs) on the slices included the cerebral cortex, hippocampus, striatum, thalamus, and cerebellum. The signal intensities in these regions are expressed as background-subtracted photo-stimulated luminescence values per square millimeter.

Statistical analysis

Statistical analysis was performed using ANOVA with StatView software. $p<0.05$ was considered significant.

Results

Physical binding of $A\beta_{1-42}$ to esRAGE

We first examined direct physical binding of human $A\beta_{1-42}$ to human esRAGE by SPR. Purified esRAGE protein bound in a concentration-dependent manner to human $A\beta_{1-42}$ immobilized onto a BIAcore sensor chip (Fig. 1A). The association rate constant (*ka*), dissociation rate constant (*kd*) and the equilibrium dissociation constant (*Kd*) of esRAGE binding to human $A\beta_{1-42}$ were calculated to be 181 M^{-1} s^{-1}, 8.12 x 10^{-6} s^{-1} and 44.9 nM, respectively; these are consistent with the previous report [8]. We also found $A\beta_{1-42}$ binding to esRAGE, which was already immobilized onto the sensor chip (Fig. 1B and C). With this condition, preincubation of either VN1 (KGAPKKPPQRLEWKLN) or VN2 (WKLNTGRTEAWKVLSPQG) peptide [6] with $A\beta_{1-42}$ led to a dose-dependent reduction in their association (Fig. 1B and C). These findings suggest that potential $A\beta_{1-42}$-binding sites reside in the immunoglobulin V type region of esRAGE. Association between $A\beta_{1-40}$ and the esRAGE was also found and both VN1 and VN2 peptides competed their bindings (data not shown). Because $A\beta_{1-42}$ has been regarded as the major cause of neurotoxicity at an early stage of AD [15], we focused on $A\beta_{1-42}$ in the subsequent experiments.

We next conducted a solid-phase reconstitution of a receptor-ligand binding and the competition assay to see whether the binding of $A\beta_{1-42}$ to RAGE was inhibited by esRAGE. The binding of FAM-labeled $A\beta_{1-42}$ to RAGE was decreased by an addition of esRAGE protein in a dose-dependent manner (Fig. 1D). The binding between two was almost completely inhibited by more than 100 μg/mL of esRAGE in this assay condition.

Creation of transgenic mice with high level of human esRAGE in circulation

We attempted to create an animal model, in which high serum concentration of human esRAGE protein is achieved, in order to test the protective potential of this variant against AD. For this, we employed the cDNA coding for human esRAGE and the murine albumin enhancer/promoter, which was expected to drive an abundant production of esRAGE proteins and to liberate them into circulation. Fig. 2A shows a schematic representation of the transgene construct. Heterogenous esRAGE Tg mice develop normally and are fertile; body weight of the esRAGE Tg was not different from that of WT for the observation period of experimentation as was the case for RAGE-null

mice (data not shown). Serum from esRAGE Tg clearly gave, but WT or RAGE-null mice-derived serum did not, the band immunoreacted with anti-human esRAGE protein antibody at 50 kDa, to which human esRAGE proteins migrated (Fig. 2B). When sera were assayed with the human esRAGE ELISA system, the mean esRAGE concentration was estimated to be 2.39 ± 0.19 μg/mL in esRAGE Tg (n= 67) (Fig. 2C). This value was more than 4 orders of magnitude higher than the mean in normal human subjects (0.13 ± 0.06 ng/mL) [35]. Human esRAGE protein was not detected either in WT or RAGE-null mice (Fig. 2C). Next we determined the levels of endogenous membrane-bound RAGE protein and transgene-derived human esRAGE in brain from WT, RAGE-null and esRAGE Tg mice using pan-RAGE antibody with which both membrane-bound RAGE and esRAGE of either human or mouse origin can be simultaneously evaluated. As shown in Fig. 2D, the membrane-bound RAGE was expressed to a similar extent in brain of WT and esRAGE Tg mice. On the other hand, human esRAGE was detected only in esRAGE Tg mice. RAGE immunoreactivity was not detected in RAGE-null mice. The results thus indicate that the murine albumin promoter-human esRAGE transgene did direct the synthesis of large amounts of circulating esRAGE.

Characterization of radiolabeled A$\beta_{1\text{-}42}$

Fig. 3A shows the elution profile of ^{125}I-labeled A$\beta_{1\text{-}42}$ in reverse-phase HPLC. When eluted with TBS being monitored by absorbance at 220 nm and by γ-ray counting, the peak was marked at 12-13 min of retention time. The fractions around the peak were collected and subjected to another reverse-phase HPLC with a 20-60% linear gradient of acetonitrile. The most ^{125}I-labeled A$\beta_{1\text{-}42}$ was recovered at 36-40% acetonitrile with a retention time at 13 min (Fig. 3B). The recovered fractions were then analyzed by SDS-PAGE and autoradiography. Before labeling, solubilized A$\beta_{1\text{-}42}$ gave a single band at less than 7 kDa in SDS-PAGE, the position to which A$\beta_{1\text{-}42}$ monomers migrated (Fig. 3C). On the same gel, the ^{125}I-labeled A$\beta_{1\text{-}42}$ was run in parallel and autoradiographed. A single band was marked at the same position as the CBB-stained cold peptides, indicating that the most ^{125}I-labeled A$\beta_{1\text{-}42}$ peptides remained in the monomeric but not the oligomeric form in this condition.

Tissue uptake and distribution of ^{125}I-labeled A$\beta_{1\text{-}42}$

Since RAGE is considered to regulate A$\beta_{1\text{-}42}$ transport and equilibrium between brain and circulation [22,23], we then administered radiolabeled A$\beta_{1\text{-}42}$ and compared

its biodistribution among WT, esRAGE Tg and RAGE-null mice. After intravenous bolus injection of ^{125}I-labeled A$\beta_{1\text{-}42}$, blood, brain, lungs, liver, gallbladder, kidneys, and urine samples were collected at various time points and γ-ray-counted. The most striking difference was observed in the brain. The brain uptake of radiolabeled A$\beta_{1\text{-}42}$ peaked at 30 min in WT mice (0.3% of injected ^{125}I-labeled A$\beta_{1\text{-}42}$), but this was blunted both in esRAGE Tg and RAGE-null mice (Fig. 4). The differences between WT and esRAGE Tg mice and between WT and RAGE-null mice were statistically significant (p<0.0001). The brain uptake at 30 min was not significantly different between esRAGE Tg and RAGE-null mice. The uptake by the lung was also less both in esRAGE Tg and RAGE-null mice at various time points than in WT controls (Fig. 4). Blood levels of ^{125}I-labeled A$\beta_{1\text{-}42}$ were essentially unchanged during the observation period by 120 min and not significantly different among WT, esRAGE Tg, and RAGE-null mice. We also examined the distribution to metabolic organs, that is, the liver and the kidney, and excretion from them (gallbladder and urine). Injected ^{125}I-labeled A$\beta_{1\text{-}42}$ seemed to be excreted into bile and urine in a time-dependent manner, but we could not detect any significant differences in the radioactivities among the three types of animals at every time point tested. However, the early liver uptake of ^{125}I-labeled A$\beta_{1\text{-}42}$ (15% of injected ^{125}I-labeled A$\beta_{1\text{-}42}$ in WT mice) was significantly decreased only in RAGE-null mice at 5 min and was significantly increased in esRAGE Tg mice at 15 min after the injection (Fig. 4). In the kidney, 38% of injected ^{125}I-labeled A$\beta_{1\text{-}42}$ was detected in WT mice at 5 min, and lower radioactivities were noted both in RAGE-null and esRAGE Tg mice at 15 and 30 min, respectively (Fig. 4).

Radiolabeled A$\beta_{1\text{-}42}$ distribution in various brain regions

We then conducted autoradiographic analysis of the brain to compare regional distribution of radiolabeled A$\beta_{1\text{-}42}$ among WT, esRAGE Tg, and RAGE-null mice. The brain was removed 30 min after intravenous injection of ^{125}I-labeled A$\beta_{1\text{-}42}$, the time point when the significant reduction in the brain uptake of ^{125}I-labeled A$\beta_{1\text{-}42}$ was observed in esRAGE Tg and RAGE-null mice. The radioactivity was highest at cerebral ventricles in WT mouse brain (Fig 5). The signals on cerebral ventricle were significantly decreased in RAGE-null and esRAGE Tg mice compared with those of WT controls. The signals on hippocampal region of RAGE-null and esRAGE Tg mice were weaker than those of WT mice. Fig. 5B shows photo-stimulated luminescence (PSL) values at various brain regions among the three types of animals. Because the values of the cerebellum were consistently similar among the three groups, the values of

the other brain regions were related to those of the cerebellum of the respective animal group. Approximately 50% less PSL was recorded in lateral, third, and fourth ventricles of RAGE-null and esRAGE Tg mice than in the ventricles of WT mice. Approximately 30% less PSL was recorded in cerebral cortex, hippocampus, striatum, and thalamus of RAGE-null and esRAGE Tg mice than in the respective regions of WT mice. The signals on putamen and CA1 and CA3 regions of hippocampus were also statistically significantly reduced in RAGE-null and esRAGE Tg mice.

Discussion

The present study has confirmed that human $A\beta_{1\text{-}42}$ can engage the multi-ligand receptor RAGE and esRAGE with high affinity (*Kd* at 44.9 nM). This was demonstrated by direct physical association of $A\beta_{1\text{-}42}$ and esRAGE (Fig. 1A, B, and C) and by the peptide competitive inhibition (Fig.1B and C), and by solid-phase reconstitution of a receptor-ligand binding and the competition assay (Fig.1D). The results are consistent with the previous reports [6, 39]. Human $A\beta_{1\text{-}42}$ binding sites of RAGE were found to be VN1 (KGAPKKPPQRLEWKLN) and VN2 (WKLNTGRTEAWKVLSPQG) regions within the immunoglobulin V type domain of RAGE. The amino acid sequences of VN1 and VN2 are well conserved between human and mouse; 93.75% sequence identity in VN1 and 100% in VN2. In disagreement with this case, we recently reported that LPS binding site of RAGE was only VN1 region, not VN2 [6]. With regard to esRAGE-binding site in $A\beta_{1\text{-}40/1\text{-}42}$, Chaney *et al.* suggested three negative charged residues (3, 7 and 11 of $A\beta_{1\text{-}40/1\text{-}42}$ sequence) of $A\beta_{1\text{-}40/1\text{-}42}$ as the most important for binding of $A\beta_{1\text{-}40/1\text{-}42}$ to RAGE by atomic force microscopy and molecular modeling [40]. Gospodarska *et al.* recently reported 17-23 (LVFFAED) residues on $A\beta_{1\text{-}40/1\text{-}42}$, a highly hydrophobic stretch flanked by negatively charged residues $D_{22}E_{23}$, were the major binding site to RAGE using intrinsic RAGE tryptophan fluorescence and mass spectrometry of non-covalent protein-ligand complexes [39].

The previous studies by Mackic *et al.* [20] and by Deane *et al*. [23] showed that the transport of circulating $A\beta_{1\text{-}42}$ into the brain is dependent on RAGE expressed at BBB. Accordingly we established for the first time a transgenic mouse line that could abundantly produce circulating esRAGE, which would capture $A\beta_{1\text{-}42}$ and prevent the amyloid accumulation in the brain. The murine albumin enhancer/promoter employed in the construction of the transgene efficiently directed the synthesis of large amounts of human esRAGE in serum (Fig. 2). Total soluble forms of mouse RAGE protein were under the detectable level in the circulation of WT control mice (data not shown), although we reported the expression of mouse esRAGE mRNA and protein in various tissues with high sensitivity techniques [41]. This suggests mouse has more predominant membrane-bound RAGE (signaling RAGE) and less soluble form of RAGE. Accordingly, we accounted WT mice to be membrane-bound RAGE expressors (RAGE >> sRAGE/esRAGE) and the esRAGE Tg mice to be esRAGE >> RAGE models. This was supported by immunoblot analysis of brain extracts from WT, RAGE-null and esRAGE Tg mice (Fig. 2D); quantitation of band intensities with Image J program revealed that esRAGE/mRAGE ratio was 0.03 in WT and 2.13 in esRAGE

Tg mice.

The resultant esRAGE Tg showed a significant reduction in brain uptake of radiolabeled $A\beta_{1-42}$ at 30 min, when the transition of $A\beta_{1-42}$ from circulation to the brain parenchyma peaked in WT mice, as did RAGE-null mice (Fig. 4). The results were comparable with a previous report that recombinant soluble RAGE as well as anti-RAGE neutralizing antibody blocked ^{125}I-Aβ brain capillary uptake and transport across BBB [23]. Since esRAGE and sRAGE have the same ligand binding domains, this study confirmed the earlier findings showing that sRAGE reduced brain Aβ levels [23]. Maximum reduction of cerebral blood flow as well as RAGE-dependent BBB transport of Aβ was observed at 30 min after intravenous injection of $A\beta_{1-40}$ [23]. This coincides with the peak levels of $A\beta_{1-42}$ in brain in the current paper, suggesting that a similar hemodynamic mechanism works in the brain receiving either $A\beta_{1-40}$ or $A\beta_{1-42}$. In the present study, the distribution of radiolabeled $A\beta_{1-42}$ into various brain regions was also investigated. This revealed significant reduction of $A\beta_{1-42}$ uptake in regions, including ventricles, cerebral cortex, hippocampus, striatum, thalamus, and putamen, in RAGE-null and esRAGE Tg mice compared with those in WT controls (Fig. 5). Among those regions, ventricles exhibited the highest accumulation of ^{125}I-$A\beta_{1-42}$ in WT mice and the most decrease in esRAGE Tg and RAGE-null animals (Fig. 5A and B). This suggests that there may be abundant or high-affinity RAGE-dependent binding sites for $A\beta_{1-42}$ in the ventricle and choroid plexus. The intense signal on ventricles might partly reflect transition of injected ^{125}I-$A\beta_{1-42}$ from bloodstream to cerebrospinal fluid. Considerable uptake rates and relative PSL/mm^2 were noted in the brain and its regions in RAGE-null as well as esRAGE Tg mice (Figs. 4 and 5).

RAGE-null mice have neither membrane-bound nor esRAGE in the brain, periphery, and endothelial surface to transport Aβ at BBB, whereas esRAGE mice have excessive esRAGE in the circulation but perhaps normal levels of membrane-bound RAGE at BBB to bind Aβ and transport Aβ. One might expect to see a difference between esRAGE Tg and RAGE-null mice in the data shown in Figs. 4 and 5. However, there seems to be no differences between esRAGE Tg and RAGE-null mice in terms of $A\beta_{1-42}$ amount detected in the brain. This may be ascribed to the higher concentration (~μg/mL) of human esRAGE in circulation far surpassing the physiologic level of mouse RAGE expressed on the surface of endothelial cells in esRAGE Tg mice. In addition, the formation of esRAGE-Aβ complexes in circulation and the prevention of membrane-bound RAGE-Aβ interaction at BBB would allow the efflux mechanism to prevail [23], thereby promoting Aβ clearance from brain in esRAGE Tg mice.

Among the organs tested, the lung of esRAGE Tg and RAGE-null mice also

showed a significant decrease in ^{125}I-labeled Aβ_{1-42} uptake (Fig. 4). The lung is known to abundantly express RAGE [41] and may have been endowed with an enriched RAGE-mediated mechanism for ligand uptake, as is the case for the BBB. On the other hand, ^{125}I-Aβ_{1-42} levels were the same and unchanged in blood during the 120 min in the WT, RAGE-null and esRAGE Tg mice (Fig. 4). This may be due to sLRP binding of Aβ in plasma [42].

The present study revealed that uptake of radiolabeled Aβ_{1-42} to CA1 and CA3 hippocampal regions was decreased by high levels of esRAGE in circulation or by RAGE deficiency (Fig. 5B). The pyramidal cells in the CA1 region are reported to be vulnerable to degeneration, and this has been related to impaired cognitive function in AD [43]. Our previous study revealed that esRAGE immunoreactivity was decreased in the same regions of hippocampus in AD brains as for non-AD brains [31]. We speculate that, in addition to low expression of esRAGE in the hippocampus, low serum esRAGE may become a risk for AD. In effect, Emanuele *et al.* reported lower plasma soluble RAGE levels in AD compared with those in non-AD patients or controls [44].

Aβ and RAGE constitute a vicious cycle of the progression in AD. Ligand engagement of RAGE activates the RAGE gene itself via activation of NF-κB, thus forming a positive loop of regulation [45,46]. Aβ has been shown to belong to the group of ligands that are able to upregulate RAGE expression [47-50]. Moreover, Aβ can induce another cascade of post-RAGE signaling; (1) an intracellular calcium mobilization activates nuclear factor activated T cells 1 (NFAT1) to upregulate beta-site APP-cleaving enzyme (BACE) expression, resulting in β-secretase-driven Aβ generation [51], (2) cytokine secretion and proinflammatory reactions [52], (3) migration of inflammatory cells across BBB [24]. We hypothesize that esRAGE can sequester Aβ_{1-42} for systemic clearance and antagonize Aβ_{1-42} binding to cell surface RAGE, blocking the amplification loop for more RAGE and Aβ_{1-42} generation on one hand, and inhibiting RAGE-mediated transport of Aβ_{1-42} into the brain on the other, thereby preventing amyloid aggregation within the brain and subsequent neuronal death.

In conclusion, evidence obtained in the present study suggests a therapeutic potential of esRAGE against AD. In addition, circulating soluble RAGE, including esRAGE, should be a useful biomarker to predict susceptibility/resistance to AD.

ACKNOWLEDGMENTS

We thank Dr. Thorgeirsson S. Sorri (National Cancer Institute) and Dr. Conner A. Elizabeth (National Cancer Institute) for providing the mouse albumin enhancer/promoter construct and Mr. Shin-ichi Matsudaira, Ms Reiko Kitamura, and Ms

Yuko Niimura for their assistance. This study has been supported by Grants-in-Aid for Scientific Research for HY from the Japan Society for the Promotion of Science (grant # 19390085 for HY; grant # 21590304 for TW) and in part by a Grant for Project Research from the High-Technology Center of Kanazawa Medical University (grant # H2010-10). The authors report no conflicts of interest.

References

[1] Schmidt AM, Vianna M, Gerlach M, Brett J, Ryan J, Kao J, Esposito C, Hegarty H, Hurley W, Clauss M, Wangll F, Pan YC, Tsang TC, Stern D (1992) Isolation and characterization of two binding proteins for advanced glycosylation end products from bovine lung which are present on the endothelial cell surface. *J Biol Chem* **267**, 14987-14997.

[2] Hofmann MA, Drury S, Fu C, Qu W, Taguchi A, Lu Y, Avila C, Kambham N, Bierhaus A, Nawroth P, Neurath MF, Slattery T, Beach D, McClary J, Nagashima M, Morser J, Stern D, Schmidt AM (1999) RAGE mediates a novel proinflammatory axis: a central cell surface receptor for S100/calgranulin polypeptides. *Cell* **97**, 889-901.

[3] Chavakis T, Bierhaus A, Al-Fakhri N, Schneider D, Witte S, Linn T, Nagashima M, Morser J, Arnold B, Preissner KT, Nawroth PP (2003) The pattern recognition receptor (RAGE) is a counterreceptor for leukocyte integrins: a novel pathway for inflammatory cell recruitment. *J Exp Med* **198**, 1507-1515.

[4] Sousa MM, Yan SD, Stern D, Saraiva MJ (2000) Interaction of the receptor for advanced glycation end products (RAGE) with transthyretin triggers nuclear transcription factor κB (NF-κB) activation. *Lab Invest* **80**, 1101-1110.

[5] Hori O, Brett J, Slattery T, Cao R, Zhang J, Chen J, Nagashima M, Lundh ER, Vijay S, Nitecki D, Morser J, Stern D, Schmidt AM (1995) The receptor for advanced glycation end products (RAGE) is a cellular binding site for amphoterin: mediation of neurite outgrowth and co-expression of rage and amphoterin in the developing nervous system. *J Biol Chem* **270**, 25752-25761.

[6] Yamamoto Y, Harashima A, Saito H, Tsuneyama K, Munesue S, Motoyoshi S, Han D, Watanabe T, Asano M, Takasawa S, Okamoto H, Shimura S, Karasawa T, Yonekura H, Yamamoto H (2011) Septic shock is associated with receptor for advanced glycation endproducts (RAGE) ligation of LPS. *J Immunol* **186**, 3248-3257.

[7] He M, Kubo H, Morimoto K, Fujino N, Suzuki T, Takahasi T, Yamada M, Yamaya M, Maekawa T, Yamamoto Y, Yamamoto H (2011) Receptor for advanced glycation end products binds to phosphatidylserine and assists in the clearance of apoptotic cells. *EMBO Rep* **12**, 358-364

[8] Yan SD, Chen X, Fu J, Chen M, Zhu H, Roher A, Slattery T, Zhao L, Nagashima M, Morser J, Migheli A, Nawroth P, Stern D, Schmidt AM (1996) RAGE and amyloid-β peptide neurotoxicity in Alzheimer's disease. *Nature* **382**, 685-691.

[9] Yamamoto Y, Kato I, Doi T, Yonekura H, Ohashi S, Takeuchi M, Watanabe T, Yamagishi S, Sakurai S, Takasawa S, Okamoto H, Yamamoto H (2001) Development

and prevention of advanced diabetic nephropathy in RAGE-overexpressing mice. *J Clin Invest* **108**, 261-268.
[10] Schmidt AM, Yan SD, Yan SF, Stern DM (2001) The multiligand receptor RAGE as a progression factor amplifying immune and inflammatory responses. *J Clin Invest* **108**, 949-955.
[11] Bucciarelli LG, Wendt T, Rong L, Lalla E, Hofmann MA, Goova MT, Taguchi A, Yan SF, Yan SD, Stern DM, Schmidt AM (2002) RAGE is a multiligand receptor of the immunoglobulin superfamily: implications for homeostasis and chronic disease. *Cell Mol Life Sci* **59**, 1117-1128.
[12] Sparvero LJ, Asafu-Adjei D, Kang R, Tang D, Amin N, Im J, Rutledge R, Lin B, Amoscato AA, Zeh HJ, Lotze MT (2009) RAGE (receptor for advanced glycation endproducts), RAGE ligands, and their role in cancer and inflammation. *J Transl Med* **7**, 7-28.
[13] Kosik KS, Duffy LK, Dowling MM, Abraham C, McCluskey A, Selkoe DJ (1984) Microtubule-associated protein 2: monoclonal antibodies demonstrate the selective incorporation of certain epitopes into Alzheimer neurofibrillary tangles. *Proc Natl Acad Sci U S A* **81**, 7941-7945.
[14] Hardy JA, Higgins GA (1992) Alzheimer's disease: the amyloid cascade hypothesis. *Science* **256**, 184-185.
[15] Giri R, Selvaraj S, Miller CA, Hofman F, Yan SD, Stern D, Zlokovic BV, KalraVK (2002) Effect of endothelial cell polarity on β-amyloid-induced migration of monocytes across normal and AD endothelium. *Am J Physiol Cell Physiol* **283**, C895-C904.
[16] Zou K, Gong JS, Yanagisawa K, Michikawa M (2002) A novel function of monomeric amyloid β-protein serving as an antioxidant molecule against metal-induced oxidative damage. *J Neurosci* **22**, 4833-4841.
[17] Zou K, Kim D, Kakio A, Byun K, Gong JS, Kim J, Kim M, Sawamura N, Nishimoto S, Matsuzaki K, Lee B, Yanagisawa K, Michikawa M (2003) Amyloid β-protein (Aβ)1–40 protects neurons from damage induced by Aβ1–42 in culture and in rat brain. *J Neurochem* **87**, 609-619.
[18] Zloković BV, Segal MB, Begley DJ, Davson H, Rakić L (1985) Permeability of the Blood-Cerebrospinal Fluid and Blood-Brain Barriers to Thyrotropin-Releasing Hormone. *Brain Res* **358**, 191-199.
[19] Mann GE, Zlokovic BV, Yudilevich DL (1985) Evidence for a lactate transport system in the sarcolemmal membrane of the perfused rabbit heart: kinetics of unidirectional influx, carrier specificity and effects of glucagon. *Biochim Biophys Acta* **819**, 241-248.

[20] Mackic JB, Stins M, McComb JG, Calero M, Ghiso J, Kim KS, Yan SD, Stern D, Schmidt AM, Frangione B, Zlokovic BV (1998) Human blood–brain barrier receptors for Alzheimer's amyloid-β 1–40. Asymmetrical binding, endocytosis, and transcytosis at the apical side of brain microvascular endothelial cell monolayer. *J Clin Invest* **102**, 734-743.

[21] Zlokovic BV, Yamada S, Holtzman D, Ghiso J, Frangione B (2000) Clearance of amyloid β-peptide from brain: transport or metabolism? *Nat Med* **6**, 718.

[22] Zlokovic BV (2004) Clearing amyloid through the blood–brain barrier. *J Neurochem* **89**, 807-811.

[23] Deane R, Du YS, Submamaryan RK, LaRue B, Jovanovic S, Hogg E, Welch D, Manness L, Lin C, Yu J, Zhu H, Ghiso J, Frangione B, Stern A, Schmidt AM, Armstrong DL, Arnold B, Liliensiek B, Nawroth P, Hofman F, Kindy M, Stern D, Zlokovic B (2003) RAGE mediates amyloid-β peptide transport across the blood–brain barrier and accumulation in brain. *Nat Med* **9**, 907-913.

[24] Giri R, Shen Y, Stins M, Du YS, Schmidt AM, Stern D, Kim KS, Zlokovic B, Kalra VK (2000) β-amyloid-induced migration of monocytes across human brain endothelial cells involves RAGE and PECAM-1. *Am J Physiol Cell Physiol* **279**, C1772-C1781.

[25] Yonekura H, Yamamoto Y, Sakurai S, Petrova RG, Abedin MJ, Li H, Yasui K, Takeuchi M, Makita Z, Takasawa S, Okamoto H, Watanabe T, Yamamoto H (2003) Novel splice variants of the receptor for advanced glycation end-products expressed in human vascular endothelial cells and pericytes, and their putative roles in diabetes-induced vascular injury. *Biochem J* **370**, 1097-1109.

[26] Hanford LE, Enghild JJ, Valnickova Z, Petersen SV, Schaefer LM, Schaefer TM, Reinhart TA, Oury TD (2004) Purification and characterization of mouse soluble receptor for advanced glycation end products (sRAGE). *J Biol Chem* **279**, 50019-50024.

[27] Raucci A, Cugusi S, Antonelli A, Barabino SM, Monti L, Bierhaus A, Reiss K, Saftig P, Bianchi ME (2008) A soluble form of the receptor for advanced glycation endproducts (RAGE) is produced by proteolytic cleavage of the membrane-bound form by the sheddase a disintegrin and metalloprotease 10 (ADAM10). *FASEB J* **10**, 3716-3727.

[28] Zhang L, Bukulin M, Kojro E, Roth A, Metz VV, Fahrenholz F, Nawroth PP, Bierhaus A, Postina R (2008) Receptor for advanced glycation end products is subjected to protein ectodomain shedding by metalloproteinases. *J Biol Chem* **283**, 35507-35516

[29] Zhang L, Postina R, Wang Y (2009) Ectodomain shedding of the receptor for advanced glycation end products: a novel therapeutic target for Alzheimer's disease.

Cell Mol Life Sci **66**, 3923-3935
[30] Cheng C, Tsuneyama K, Kominami R, Shinohara H, Sakurai S, Yonekura H, Watanabe T, Takano Y, Yamamoto H, Yamamoto Y (2005) Expression profiling of endogenous secretory receptor for advanced glycation end products in human organs. *Mod Pathol* **18**, 1385-1396.
[31] Nozaki I, Watanabe T, Kawaguchi M, Akatsu H, Tsuneyama K, Yamamoto Y, Ohe K, Yonekura H, Yamada M, Yamamoto H (2007) Reduced expression of endogenous secretory receptor for advanced glycation endproducts in hippocampal neurons of Alzheimer's disease brains. *Arch Histol Cytol* **70**, 1691-1696.
[32] Conner EA, Lemmer ER, Omori M, Wirth PJ, Factor VM, Thorgeirsson SS (2000) Dual functions of E2F-1 in a transgenic mouse model of liver carcinogenesis. *Oncogene* **19**, 5054-5062.
[33] Myint KM, Yamamoto Y, Doi T, Kato I, Harashima A, Yonekura H, Watanabe T, Shinohara H, Takeuchi M, Tsuneyama K, Hashimoto N, Asano M, Takasawa S, Okamoto H, and Yamamoto H (2006) RAGE control of diabetic nephropathy in a mouse model: effects of RAGE gene disruption and administration of low-molecular weight heparin. *Diabetes* **55**, 2510-2522.
[34] Sakatani S, Yamada K, Homma C, Munesue S, Yamamoto Y, Yamamoto H, Hirase H (2009) Deletion of RAGE causes hyperactivity and increased sensitivity to auditory stimuli in mice. *PLoS One* **4**, e8309.
[35] Sakurai S, Yamamoto Y, Tamei H, Matsuki H, Obata K, Hui L, Miura J, Osawa M, Uchigata Y, Iwamoto Y, Watanabe T, Yonekura H, Yamamoto H (2006) Development of an ELISA for esRAGE and its application to type 1 diabetic patients. *Diabetes Res Clin Pract* **73**, 158-165.
[36] Poduslo JF, Curran GL, Berg CT (1994) Macromolecular permeability across the blood-nerve and blood-brain barriers. *Proc Natl Acad Sci USA* **91**, 5705-5709.
[37] Zlokovic BV, Martel CL, Matsubara E, McComb JG, Zheng G, McCluskey RT, Frangione B, Ghiso J (1996) Glycoprotein 330/ megalin: probable role in receptor-mediated transport of apolipoprotein J alone and in a complex with Alzheimer disease amyloid β at the blood–brain and blood–cerebrospinal fluid barriers. *Proc Natl Acad Sci USA* **93**, 4229-4234.
[38] Martel CL, Mackic JB, Matsubara E, Governale S, Miguel C, Miao W, McComb JG, Frangione B, Ghiso J, Zlokovic BV (1997) Isoform-specific effects of apolipoproteins E2, E3, and E4 on cerebral capillary sequestration and blood-brain barrier transport of circulating Alzheimer's amyloid β. *J Neurochem* **69**, 1995-2004.
[39] Gospodarska E, Kupniewska-Kozak A, Goch G, Dadlez M (2011) Binding studies

of truncated variants of the Aβ peptide to the V-domain of the RAGE receptor reveal Aβ residues responsible for binding. *Biochim Biophys Acta* **1814**, 592-609

[40] Chaney MO, Stine WB, Kokjohn TA, Kuo YM, Esh C, Rahman A, Luehrs DC, Schmidt AM, Stern D, Yan SD, Roher AE (2005) RAGE and amyloid beta interactions: atomic force microscopy and molecular modeling. *Biochim Biophys Acta* **1741**, 199-205.

[41] Harashima A, Yamamoto Y, Cheng C, Tsuneyama K, Myint KM, Takeuchi A, Yoshimura K, Li H, Watanabe T, Takasawa S, Okamoto H, Yonekura H, Yamamoto H (2006) Identification of mouse orthologue of endogenous secretory receptor for advanced glycation end-products: structure, function and expression. *Biochem J* **396**, 109-115.

[42] Sagare A, Deane R, Bell RD, Johnson B, Hamm K, Pendu R, Marky A, Lenting PJ, Wu Z, Zarcone T, Goate A, Mayo K, Perlmutter D, Coma M, Zhong Z, Zlokovic BV (2007) Clearance of amyloid-β by circulating lipoprotein receptors. *Nat Med* **9**, 1029-1031.

[43] West MJ, Kawas CH, Stewart WF, Rudow GL, Troncoso JC (2004) Hippocampal neurons in pre-clinical Alzheimer's disease. *Neurobiol Aging* **25**, 1205-1212.

[44] Emanuele E, D'Angelo A, Tomaino C, Binetti G, Ghidoni R, Politi P, Bernardi L, Maletta R, Bruni AC, Geroldi D (2005) Circulating levels of soluble receptor for advanced glycation end products in Alzheimer disease and vascular dementia. *Arch Neurol* **62**, 1734–1736.

[45] Tanaka N, Yonekura H, Yamagishi S, Fujimori H, Yamamoto Y, Yamamoto H (2000) The receptor for advanced glycation endproducts is induced by the glycation products themselves and TNF-α through NF-κB, and by 17β-estradiol through Sp-1 in human vascular endothelial cells. *J Biol Chem* **275**, 25781-25790.

[46] Lander HM, Tauras JM, Ogiste JS, Hori O, Moss RA, Schmidt AM (1997) Activation of the receptor for advanced glycation end products triggers a p21(ras)-dependent mitogen-activated protein kinase pathway regulated by oxidant stress. *J Biol Chem* **272**, 17810-17814.

[47] Li J, Schmidt AM (1997) Characterization and functional analysis of the promoter of RAGE, the receptor for advanced glycation end products. *J Biol Chem* **272**, 16498-16506.

[48] Li JJ, Dickson D, Hof PR, Vlassara H (1998) Receptors for advanced glycosylation endproducts in human brain: role in brain homeostasis. *Mol Med* **4**, 46-60.

[49] Bierhaus A, Schiekofer S, Schwaninger M, Andrassy M, Humpert PM, Chen J, Hong M, Luther T, Henle T, Klöting I, Morcos M, Hofmann M, Tritschler H, Weigle B,

Kasper M, Smith M, Perry G, Schmidt AM, Stern DM, Häring HU, Schleicher E, Nawroth PP (2001) Diabetes-associated sustained activation of the transcription factor nuclear factor-kappaB. *Diabetes* **50**, 2792-2808.
[50] Stern DM, Schmidt AM, Yan SD, Yan SF (2002) Receptor for advanced glycation endproducts (RAGE) and the complications of diabetes. *Ageing Res Rev* **1**, 1-15.
[51] Cho HJ, Son SM, Jin SM, Hong HS, Shin DH, Kim SJ, Huh K, Mook-Jung I (2009) RAGE regulates BACE1 and Aβ generation via NFAT1 activation in Alzheimer's disease animal model. *FASEB J* **23**, 2639-2649.
[52] Li M, Shang DS, Zhao WD, Tian L, Li B, Fang WG, Zhu L, Man SM, Chen YH (2002) Amyloid β interaction with receptor for advanced glycation end products up-regulates brain endothelial CCR5 expression and promotes T cells crossing the blood-brain barrier. *J Immunol* **182**, 5778-5788.

Figure legends

Figure 1

Binding of $A\beta_{1\text{-}42}$ to esRAGE and its competition by synthetic peptides of RAGE.

(A) Surface plasmon resonance (SPR) analysis. esRAGE at varying concentrations was perfused onto an $A\beta_{1\text{-}42}$-immobilized BIAcore sensor chip. Thirty seconds after the injection, the mobile phase was changed back to the buffer without the analyte. (B, C) SPR assays. Thirty μg/mL of $A\beta_{1\text{-}42}$ was perfused on the extracellular domain of RAGE immobilized on a sensor chip. Thirty seconds after the injection, the mobile phase was changed back to the buffer without $A\beta_{1\text{-}42}$. For competition assay, the same concentration of $A\beta_{1\text{-}42}$ was preincubated with the indicated concentrations equal to or in excess of VN1 or VN2 peptide for 30 min, and the preincubation mixtures were injected into the sensor chip on which esRAGE had been immobilized. (D) esRAGE immobilized to a 96-well plate was incubated with FAM-labeled $A\beta_{1\text{-}42}$ in the presence or absence of indicated concentrations of esRAGE for 1 hr and the intensity of fluorescence was detected at exitation/emission = 495/521 nm.

Figure 2

Generation and characterization of human esRAGE-overexpressing mice.

(A) Schematic diagram of the transgene carrying human esRAGE cDNA under the control of mouse albumin enhancer/promoter. The construct also has human β-globin intron and SV40 late poly(A) signal (SV40 Poly A). Alb, albumin; Enh, enhancer; Pr, promoter. Hga-I, *Hga*-I site for restriction. (B) Immunoblot analysis of sera from wild-type (WT), RAGE-null (KO), and esRAGE Tg (TG) mice with anti-human esRAGE antibody. (C) Serum human esRAGE concentrations were determined by ELISA in wild-type (WT), RAGE-null (KO) and esRAGE Tg (TG) mice. Data are expressed as mean ± SEM. n.d., not detected. (D) Immunoblot analysis of brain tissues from wild-type (WT), RAGE-null (KO) and esRAGE Tg (TG) mice with pan-RAGE antibody (upper panel) and human esRAGE-specific antibody (lower panel). mRAGE, membrane-bound RAGE.

Figure 3

HPLC separation and characterization of radiolabeled $A\beta_{1\text{-}42}$ peptide.

(A) Chromatography on a Zorbax 300 Extend-C18 column equilibrated and eluted with TBS, pH 7.4. The ordinate shows absorbance at 220 nm. Bar, the peak fractions collected for further purification. (B) Chromatography on a Zorbax 300 Extend-C18 column using a 20-60% linear gradient of acetonitrile in 0.1% TFA. The ordinate,

absorbance at 220 nm; bar, the peak fractions collected. (C) SDS-PAGE analysis of $A\beta_{1-42}$ peptides before and after ^{125}I-labeling. One μg of $A\beta_{1-42}$ peptides was electrophoresed on 5-20% gradient polyacrylamide gel and stained with Coomassie brilliant blue (CBB). 5,000 cpm of ^{125}I-labeled peptides was run on the same gel and autoradiographed. Prestained SDS-PAGE standard broad range was used as calibration markers.

Figure 4

Tissue distribution of radiolabeled $A\beta_{1-42}$ in wild-type (WT), RAGE-null (KO) and esRAGE Tg (TG) mice. Animals received intravenous bolus injection of 2 μCi of ^{125}I-labeled $A\beta_{1-42}$ peptides in 0.2 mL of 0.1% BSA solution, and euthanized at indicated time points. After blood was drawn, mice were perfused with PBS, and tissues were removed, weighed, and processed for γ-counting. Values are expressed as % dose/g wet tissue. Data are expressed as mean ± SEM. *, $p<0.05$; **, $p<0.02$; $^{\#}$, $p<0.0001$ compared with the value of WT control at each time point. Values for blood were calculated under the assumption that blood constitutes 7% of the total body weight.

Figure 5

Distribution of ^{125}I-labeled $A\beta_{1-42}$ within the brains of wild-type (WT), RAGE-null (KO) and esRAGE Tg (TG) mice. (A) Typical autoradiograms of horizontal sections. LV, lateral ventricle; HIP, hippocampus. (B) Comparison of radiolabeled $A\beta_{1-42}$ distributions in various brain regions. Data are expressed as mean ± SEM (n=3) of relative photo-stimulated luminescence (PSL)/mm^2. Values are related to those of the cerebellum of each animal group; 1.0 in WT was equivalent to 51.7 PSL/mm^2; 1.0 in RAGE-null mice was to 52.3 PSL/mm^2; 1.0 in esRAGE Tg to 54.7 PSL/mm^2. Lat. Vent., lateral ventricle: 3rd Vent., third ventricle; 4th Vent., fourth ventricle; CTX, frontal cortex; HIP, hippocampus; STR, striatum; THA, thalamus; CA1, CA1 region of HIP; CA2, CA2 region of HIP; CA3, CA3 region of HIP; CA4, CA4 region of HIP; DG, dentate gyrus. *, $p < 0.03$; **, $p < 0.005$; $^{\#}$, $p < 0.0001$ compared with wild-type control.

Fig.1

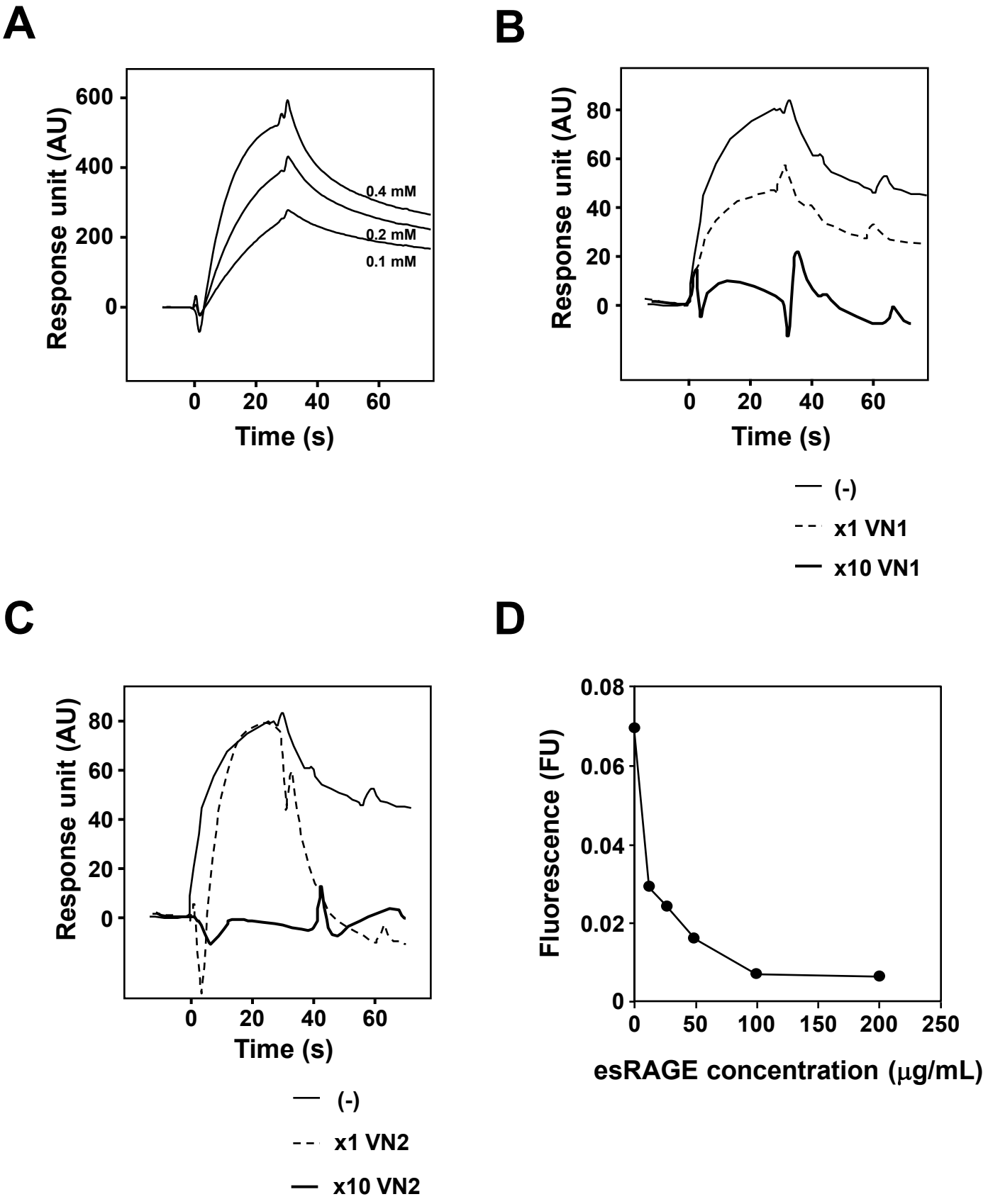
A
Response unit (AU)
600
400
200
0
0.4 mM
0.2 mM
0.1 mM
0
20
40
60
Time (s)
B
Response unit (AU)
80
60
40
20
0
0
20
40
60
Time (s)
(-)
x1 VN1
x10 VN1
C
Response unit (AU)
80
60
40
20
0
0
20
40
60
Time (s)
(-)
x1 VN2
x10 VN2
D
Fluorescence (FU)
0.08
0.06
0.04
0.02
0
0
50
100
150
200
250
esRAGE concentration (μg/mL)

Fig.2

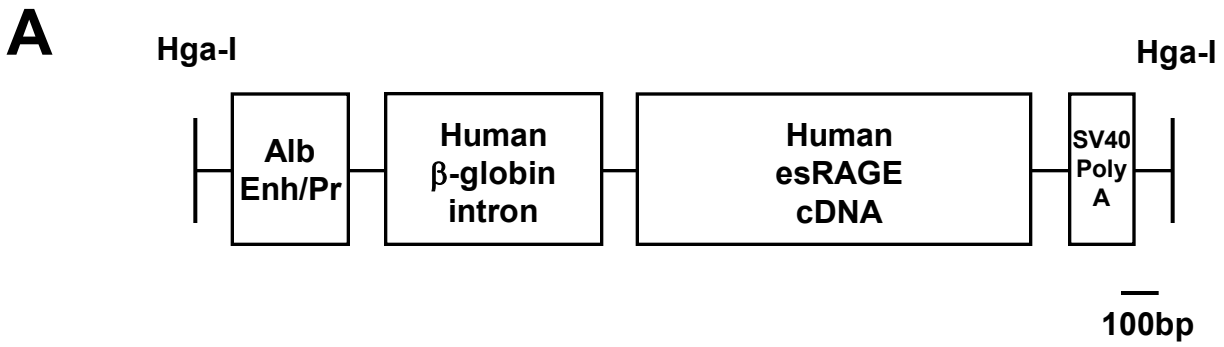
A
Hga-I
Hga-I
Alb Enh/Pr
Human β-globin intron
Human esRAGE cDNA
SV40 Poly A
100bp

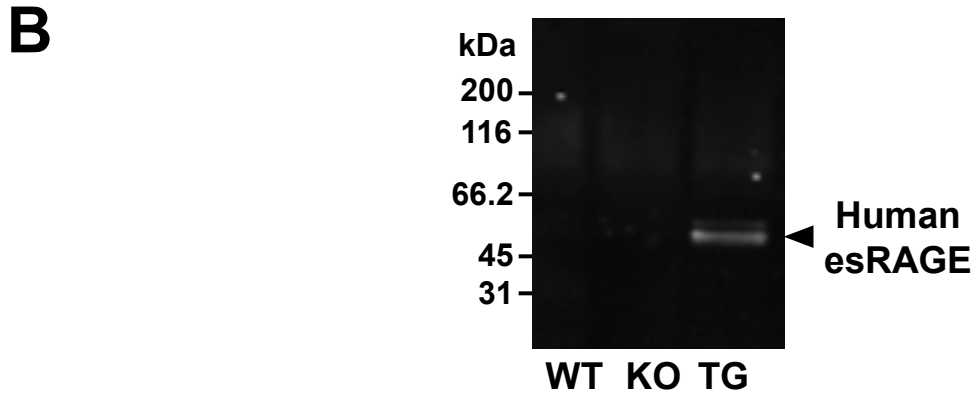
B
kDa
200
116
66.2
45
31
Human esRAGE
WT KO TG

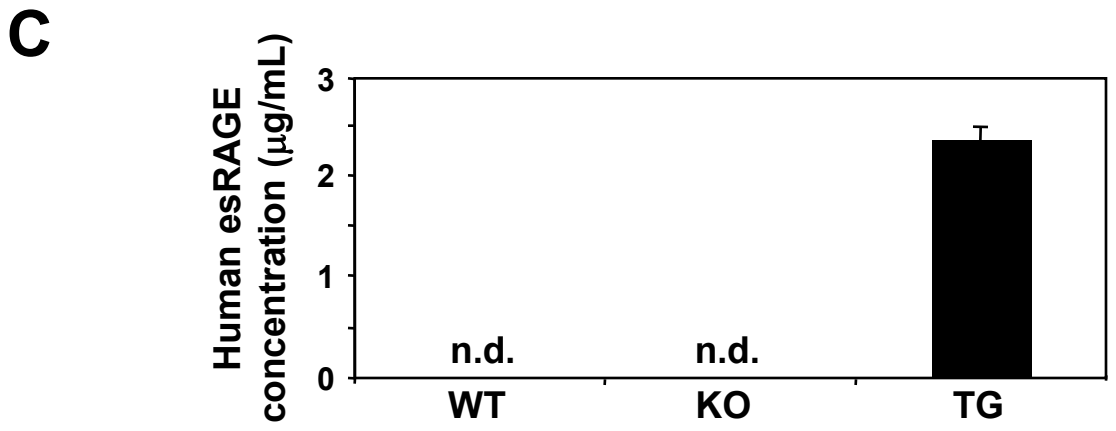
C
Human esRAGE concentration (μg/mL)
3
2
1
0
n.d.
n.d.
WT
KO
TG

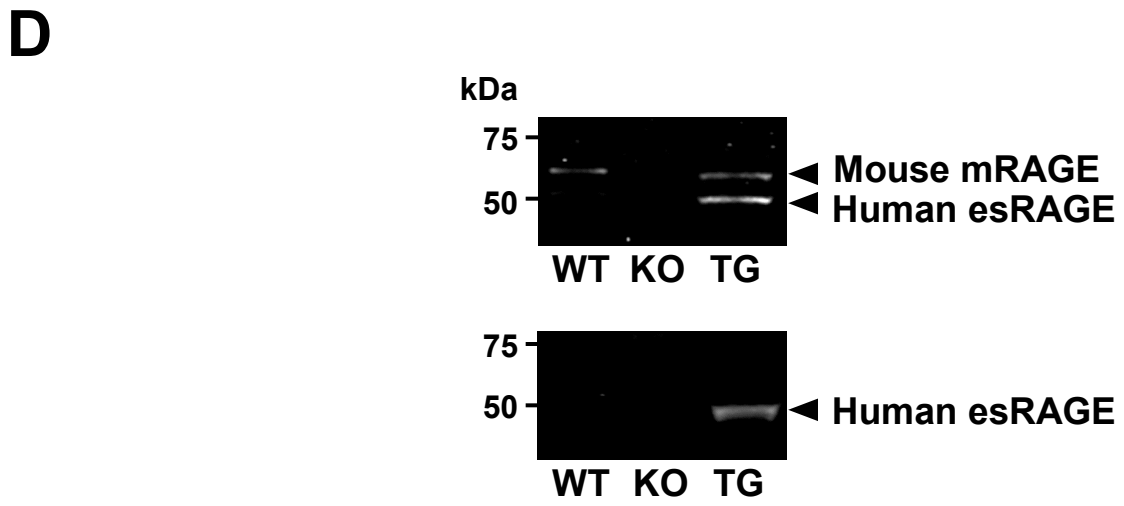
D
kDa
75
50
Mouse mRAGE
Human esRAGE
WT KO TG
75
50
Human esRAGE
WT KO TG

Fig.3

A

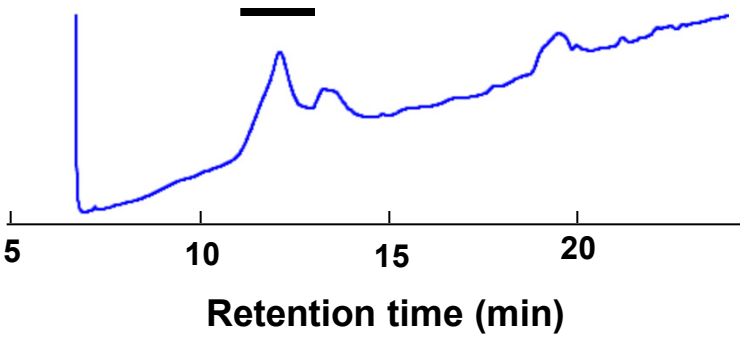
5
10
15
20
Retention time (min)

B

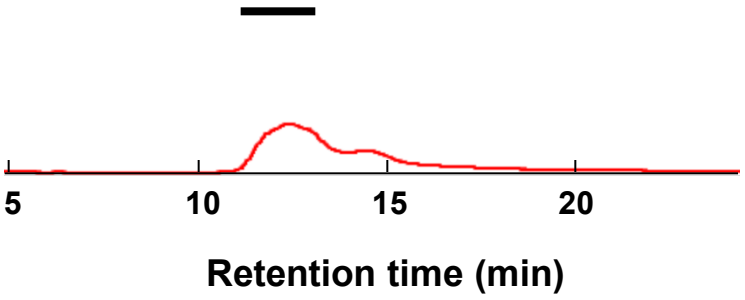
5
10
15
20
Retention time (min)

C

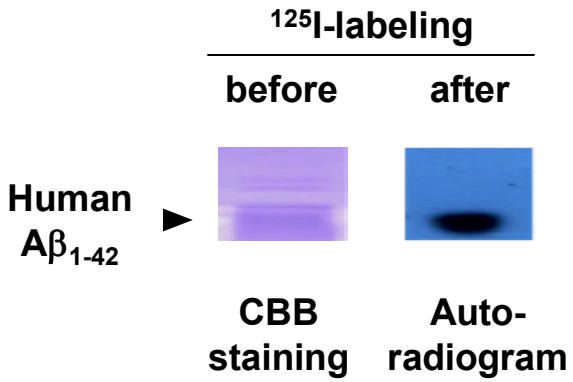
125I-labeling
before
after
Human
Aβ1-42
CBB
staining
Auto-
radiogram

Fig.4

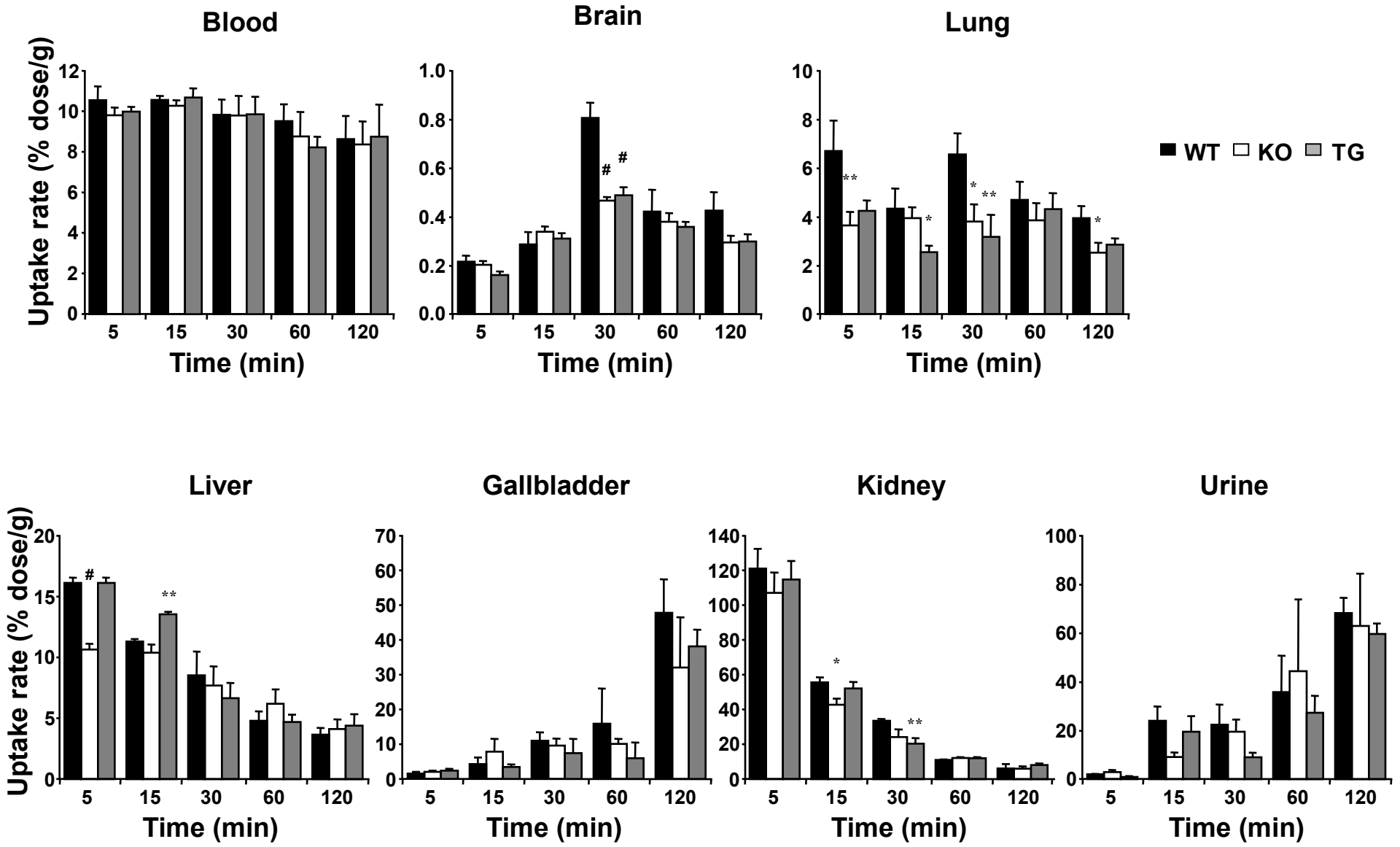
Blood
Brain
Lung
Liver
Gallbladder
Kidney
Urine
Uptake rate (% dose/g)
Time (min)
5
15
30
60
120
WT
KO
TG
#
**
*

Fig.5

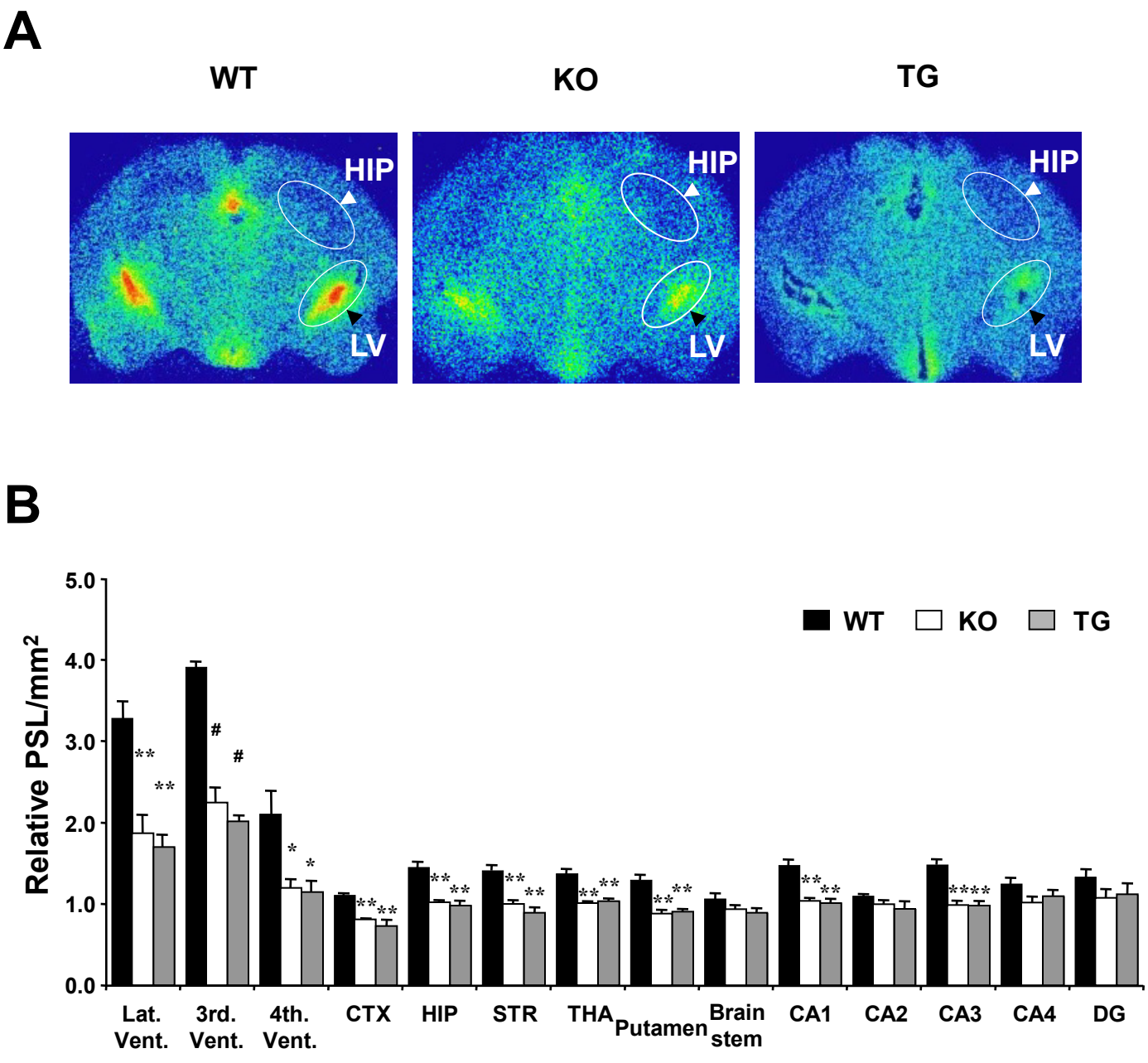
A
WT
KO
TG
HIP
LV
HIP
LV
HIP
LV
B
Relative PSL/mm2
5.0
4.0
3.0
2.0
1.0
0.0
WT
KO
TG
Lat. Vent.
3rd. Vent.
4th. Vent.
CTX
HIP
STR
THA
Putamen
Brain stem
CA1
CA2
CA3
CA4
DG